Novel Closed-Form Green's Function in Shielded Planar Layered Media

Andreas C. Cangellaris, *Fellow, IEEE,* and Vladimir I. Okhmatovski, *Member, IEEE*

***Abstract*—A new method is proposed for the construction of closed-form Green's function in planar, stratified media between two conducting planes. The new approach does not require the a priori extraction of the guided-wave poles and the quasi-static part from the Green function spectrum. The proposed methodology can be easily applied to arbitrary planar media without any restriction on the number of layers and their thickness. Based on the discrete solution of one-dimensional ordinary differential equations for the spectral-domain expressions of the appropriate vector potential components, the proposed method leads to the simultaneous extraction of all Green's function values associated with a given set of source and observation points. Krylov subspace model order reduction is used to express the generated closed-form Green's function representation in terms of a finite sum involving a small number of Hankel functions. The validity of the proposed methodology and the accuracy of the generated closed-form Green's functions are demonstrated through a series of numerical experiments involving both vertical and horizontal dipoles.**

***Index Terms*—Green's function, layered media.**

I. Introduction

INTEGRAL equation methods constitute one of the most popular classes of methods used for the electromagnetic analysis of integrated circuits and printed antennas [1], [2]. The computational efficiency and the versatility of such methods is strongly dependent on the ease with which the Green's functions associated with the background layered medium are calculated. Consequently, a significant amount of research work has been dedicated to the development of Green's functions in stratified media over the years [3]–[5]. In particular, various techniques have been proposed to overcome the high computational cost associated with the numerical evaluation of the so-called Sommerfeld integrals in terms of which the Green's function appears [6]. Among these methods, the most popular are interpolation and tabulation schemes [7]–[9]; fast Hankel transform methods [10], [11]; the steepest descent path approach [12]; and the discrete complex image method (DCIM) [13]–[15]. Since the latter seems to have received significant attention in recent years, we choose to highlight some of its attributes and will use it as the reference solution approach for our investigation.

The main advantage of DCIM is that it casts the Green's function in a simple closed form. To achieve this, first the spectral-domain form of the Green's function is fitted by a finite sum of complex exponentials using either the generalized pencil of function [16] or Prony's method [17]. Subsequently, the Sommerfeld identity [3] is applied to reduce the Sommerfeld integrals to a set of complex images. The first stage of the DCIM, associated with the fitting of the spectrum of the Green's function by exponentials, turns out to be its most sensitive part. The reason for this is that for such complex exponential fitting to be effective, the function needs to be smooth and fast decaying for large values of the spectral variable. This implies that all poles associated with the propagating waves and the quasi-static part must be extracted from the spectrum prior to fitting. Such an extraction is relatively simple to perform when the stratified medium is composed of one or two layers. However, it becomes cumbersome for the case of multilayered media. In this case, one must make use of some iterative schemes for locating the poles in the complex plane and calculating the corresponding residues [18]. There have been some attempts to avoid the extraction of propagating waves. The approach proposed in [5] proved to be very efficient and robust, but only for the case of thin layers where the propagating wave contribution is insignificant. Further investigations [19] showed that for thick layers, a large error occurs in the far field if the propagating modes are not extracted. The physical explanation is that use of complex images is in fact an attempt to approximate the cylindrical nature of propagating waves in terms of spherical ones. In [14], this difficulty was overcome by implementing Hankel functions in order to describe propagating modes and complex images for the decaying part of the field.

In this paper, an alternative to DCIM is presented. The new approach is based on the replacement of the analytic forms of the spectral-domain Green's function with discrete ones, obtained from a finite-difference solution of the governing differential equations for the pertinent vector potential components. This formulation is then combined with a computationally efficient eigenvalue analysis of the resulting finite-difference sparse matrix to represent the vector potential components as a sum of pole-residue terms, reminiscent of the extracted propagating wave contributions in DCIM. This pole-residue form of the Green's function spectrum allows the analytic evaluation of the Sommerfeld integrals, thus yielding a finite sum of Hankel functions as the spatial form for the Green's function. Further model order reduction [20] truncates this sum to one involving a small number of terms corresponding to the dominating eigenvalues. For the purposes of this paper, the new methodology is presented for the shielded stripline configuration of Fig. 1. The case of unshielded stratified media will be discussed in a forthcoming paper.

Manuscript received March 2, 2000; revised August 21, 2000.

The authors are with the Center for Computational Electromagnetics, Department of Electrical and Computer Engineering, University of Illinois at Urbana-Champaign, Urbana, IL 61801 USA.

Publisher Item Identifier S 0018-9480(00)10709-4.

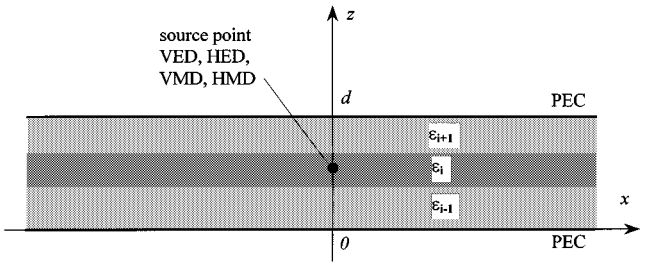

Fig. 1. Geometry of a layered dielectric medium shielded by two conducting planes.

II. The Case of Vertical Dipole Excitation

The boundary value problem of interest is shown in Fig. 1, where either a vertical electric dipole (VED) or a vertical magnetic dipole (VMD) is present at the source point z'. It is assumed that the medium can be lossy, with permeability of free space and complex permittivity varying in the vertical direction only, $\overline{\varepsilon}(x,y,z)=\overline{\varepsilon}(z)$. A z-directed electric or magnetic dipole excites only transverse magnetic to z (TM_z) or transverse electric to z (TE_z) modes, respectively. In both cases, the z-component of either the electric or the magnetic vector potential $A_z^{e,m}$ suffices to satisfy the boundary conditions. For the purposes of this paper, the time dependence is assumed to be $e^{i\omega t}$ and is suppressed for simplicity ($i=\sqrt{-1}$). The governing equation for the z-component of the vector potential is the scalar Helmholtz equation

$$\nabla^2 A_z^{e,m}+k^2 A_z^{e,m}=-j_z^{e,m} \tag{1}$$

where $k^2=\omega^2\mu_0\overline{\varepsilon}(z)$. The electromagnetic fields are given by [3]

$$\mathbf{E}=\frac{1}{i\omega\overline{\varepsilon}}\left(\nabla\nabla\cdot\mathbf{A}^e+k^2\mathbf{A}^e\right)-\nabla\times\mathbf{A}^m \tag{2}$$

$$\mathbf{H}=\frac{1}{i\omega\mu_o}\left(\nabla\nabla\cdot\mathbf{A}^m+k^2\mathbf{A}^m\right)+\nabla\times\mathbf{A}^e. \tag{3}$$

Since the material properties are independent of x and y, $A_z^{e,m}$ may be written in terms of their Fourier-Bessel transforms, utilizing the following transform pair:

$$\hat{A}_z^{e,m}(\lambda,z,z')=\int_0^\infty A_z^{e,m}(\rho,z,z')J_0(\lambda\rho)\rho\,d\rho \tag{4a}$$

$$A_z^{e,m}(\rho,z,z')=\int_0^\infty \hat{A}_z^{e,m}(\lambda,z,z')J_0(\lambda\rho)\lambda\,d\lambda \tag{4b}$$

where λ is the spectral variable. Substitution of (4b) into (1) and use of the result

$$\frac{1}{r}\,\delta(r)\delta(\varphi)=\frac{1}{2\pi}\int_0^{+\infty} J_0(\lambda r)\lambda\,d\lambda \tag{5}$$

reduces the Helmholtz equation (1) to an ordinary second-order equation for the spectrum $\hat{A}_z^{e,m}$

$$\frac{d^2\hat{A}_z^{e,m}}{dz^2}+(k^2-\lambda^2)\hat{A}_z^{e,m}=-\frac{I^{e,m}l}{2\pi}\,\delta(z-z'). \tag{6}$$

From (2) and (3), the appropriate boundary conditions for the spectra at an interface located at z_i are

$$\left.\frac{d\hat{A}_z^{e,m}}{dz}\right|_{\substack{z=0\\z=d}}=0 \tag{7}$$

$$\left.\hat{A}_z^{e}\right|_{z=z_i-}=\left.\hat{A}_z^{e}\right|_{z=z_i+} \tag{8}$$

$$\frac{1}{\varepsilon_{i-1}}\left.\frac{d\hat{A}_z^{e}}{dz}\right|_{z=z_i-}=\frac{1}{\varepsilon_i}\left.\frac{d\hat{A}_z^{e}}{dz}\right|_{z=z_i+} \tag{9}$$

$$\left.\hat{A}_z^{m}\right|_{\substack{z=0\\z=d}}=0 \tag{10}$$

$$\left.\hat{A}_z^{m}\right|_{z=z_i-}=\left.\hat{A}_z^{m}\right|_{z=z_i+} \tag{11}$$

$$\left.\frac{d\hat{A}_z^{m}}{dz}\right|_{z=z_i-}=\left.\frac{d\hat{A}_z^{m}}{dz}\right|_{z=z_i+}. \tag{12}$$

Next, a discrete approximation of (6) is developed using the finite difference method. For this purpose, the interval $z\in[0,d]$ is divided into $N-1$ elements so that a grid point with index 0 is located at the bottom ground plane and a grid point with index $N-1$ at the top plane. Use of a central difference approximation of the second-order derivative yields the following discrete form of (6) for the qth grid point that does not coincide with a media interface:

$$\frac{\hat{A}_z^{e,m}(z_{q+1})-2\hat{A}_z^{e,m}(z_q)+\hat{A}_z^{e,m}(z_{q-1})}{h^2}+(k_0^2\varepsilon-\lambda^2)\hat{A}_z^{e,m}(z_q)=-\frac{I^{e,m}l}{2\pi h}\,\delta_{q,q'} \tag{13}$$

where $\delta_{q,q'}$ is Kroneker's delta, q' is the grid point, at which a source is present, $k_0^2=\omega^2\mu_0\varepsilon_0$, ε is the relative permittivity of the layer, in which the grid node resides, and h is the grid size in the finite-difference grid. Without loss of generality, a uniform finite difference discretization is assumed for the sake of simplicity of the mathematical formulation.

Boundary conditions (7) at the conducting planes for $\hat{A}_z^e$ are imposed by replacing the finite difference terms in (13) for the edge elements $q=1$ and $q=N-2$ by

$$\frac{\hat{A}_z^e(z_{q+1})-\hat{A}_z^e(z_q)}{h^2} \tag{14}$$

and

$$\frac{-\hat{A}_z^e(z_q)+\hat{A}_z^e(z_{q-1})}{h^2} \tag{15}$$

respectively.

The boundary conditions (8) and (9) at layer interfaces where the permittivity is discontinuous require some care. The reason for this is that the homogeneous equation

$$\frac{d^2\hat{A}_z^e}{dz^2}+(k^2-\lambda^2)\hat{A}_z^e=0 \tag{16}$$

is not valid at the interface node since the first derivative of $\hat{A}_z^e$ is discontinuous and the second derivative produces unbalanced δ-function in the left-hand side. To handle this discontinuity, only the boundary condition (9) is enforced at the interface node. More specifically, a discrete form of (9) is used to express the value at the interface node in terms of the values of the two adjacent nodes, and the interface node is thus excluded from the discrete problem. To illustrate, let $z=z_q$ be the interface point between layers with relative permittivities ε_+ and ε_- above and

below the interface, respectively. Using a finite difference approximation of the boundary condition (9)

$$\frac{1}{\varepsilon_-}\,\frac{\hat{A}_z^e(z_q)-\hat{A}_z^e(z_{q-1})}{h}=\frac{1}{\varepsilon_+}\,\frac{\hat{A}_z^e(z_{q+1})-\hat{A}_z^e(z_q)}{h} \tag{17}$$

the following expression for $\hat{A}_z^e(z_q)$ is obtained:

$$\hat{A}_z^e(z_q)=\frac{\varepsilon_-}{\varepsilon_-+\varepsilon_+}\,\hat{A}_z^e(z_{q+1})+\frac{\varepsilon_+}{\varepsilon_-+\varepsilon_+}\,\hat{A}_z^e(z_{q-1}). \tag{18}$$

Use of (18) in (13) for the two nodes above and below the interface point $z=z_q$ yields, respectively

$$\frac{\hat{A}_z^e(z_{q+2})-2\hat{A}_z^e(z_{q+1})+\left[\dfrac{\varepsilon_-\hat{A}_z^e(z_{q+1})}{\varepsilon_-+\varepsilon_+}+\dfrac{\varepsilon_+\hat{A}_z^e(z_{q-1})}{\varepsilon_-+\varepsilon_+}\right]}{h^2}+(k_0^2\varepsilon_+-\lambda^2)\hat{A}_z^e(z_{q+1})=0 \tag{19}$$

and

$$\frac{\left[\dfrac{\varepsilon_-\hat{A}_z^e(z_{q+1})}{\varepsilon_-+\varepsilon_+}+\dfrac{\varepsilon_+\hat{A}_z^e(z_{q-1})}{\varepsilon_-+\varepsilon_+}\right]-2\hat{A}_z^e(z_{q-1})+\hat{A}_z^e(z_{q-2})}{h^2}+(k_0^2\varepsilon_--\lambda^2)\hat{A}_z^e(z_{q-1})=0. \tag{20}$$

Clearly, continuity of potential (8) is satisfied automatically when (9) is written in discrete form (17).

Application of the boundary condition (10) is straightforward by simply setting to zero the terms in the finite-difference approximation of the second derivative in (13) corresponding to the end nodes. This yields the modified finite-difference equations for the second-order derivatives in the discrete equations for nodes $q=1$ and $q=N-2$, respectively

$$\frac{\hat{A}_z^e(z_{z+1})-2\hat{A}_z^e(z_q)}{h^2} \tag{21}$$

$$\frac{-2\hat{A}_z^e(z_q)+\hat{A}_z^e(z_{q-1})}{h^2}. \tag{22}$$

The continuity of $\hat{A}_z^m$ at dielectric interfaces yields the following modified form of the discrete equation for a node q residing at the interface

$$\frac{\hat{A}_z^m(Z_{q+1})-2\hat{A}_z^m(Z_q)+\hat{A}_z^m(Z_{q-1})}{h^2}+\left(k_o^2\cdot\frac{E_++E_-}{2}-\lambda^2\right)\hat{A}_z^m(Z-q)=\frac{-I_z^m\cdot l}{2\pi h}\times\delta_{q,q'}. \tag{23}$$

It is important to point out that in (23) boundary condition (12) was also enforced since the continuity of the derivative of $\hat{A}_z^m$ is needed for (23) to be valid.

The resulting system of discrete equations for all nodes in the finite-difference grid may be cast in the compact form

$$(\mathbf{A}+\lambda^2\mathbf{I})\mathbf{x}=\mathbf{Fu} \tag{24}$$

where the matrix $\mathbf{A}$ is a tridiagonal matrix of dimension N equal to the number of discrete unknowns at the grid points, $\mathbf{I}$ is the identity matrix, and the vector $\mathbf{x}$ contains the values of the spectral-domain vector potentials $\hat{A}_z^{e,m}$ at the finite-difference nodes. For the TE_z case, $\hat{A}_z^m$ is zero on the perfectly conducting walls, and these values are not included in the vector $\mathbf{x}$. For the TM_z case, $\hat{A}_z^e$ is nonzero at $z=0$, d, and the vector of unknowns $\mathbf{x}$ contains the values of the spectral-domain Green's function at these points.

As far as the right-hand side of (24) is concerned, its form reflects the fact that it accounts for all planes in the domain where (source) dipoles are placed. To elaborate, let Q_S be the number of z planes in the domain where dipoles are present. A typical method-of-moments approximation of the boundary value problem requires the calculation of the spectral Green's function at Q_P planes due to each of the Q_S sources. In other words, a $Q_P\times Q_S$ matrix of spectral Green's functions is required. The vector $\mathbf{u}$ in (24) is of length Q_S, identifying the Q_S source planes. The matrix $\mathbf{F}$ is an $N\times Q_S$ matrix, with only one nonzero element per column. More specifically, for the qth source plane, a nonzero element of value 1 exists at the qth column of the matrix $\mathbf{F}$ and at the row corresponding to the node number in the finite-difference grid assigned to the specific source plane vector $\mathbf{x}$ is obtained formally from (24) as

$$\mathbf{x}=(\mathbf{A}+\lambda^2\mathbf{I})^{-1}\mathbf{Fu}. \tag{25}$$

Using the eigen-decomposition [22] of the matrix $\mathbf{A}$

$$\mathbf{A}=\mathbf{TST}^{-1} \tag{26}$$

where the columns of $\mathbf{T}$ are the eigenvectors of $\mathbf{A}$ and $\mathbf{S}$ is a diagonal matrix of the eigenvalues of $\mathbf{A}$, $\mathbf{x}$ may be cast in the following form:

$$\begin{aligned}\mathbf{x}&=(\mathbf{A}+\lambda^2\mathbf{I})^{-1}\mathbf{Fu}=(\mathbf{T}(\mathbf{S}+\lambda^2\mathbf{I})\mathbf{T}^{-1})^{-1}\mathbf{Fu}\\&=\mathbf{T}(\mathbf{S}+\lambda^2\mathbf{I})^{-1}\mathbf{T}^{-1}\mathbf{Fu}.\end{aligned} \tag{27}$$

Finally, the matrix $\mathbf{X}$ containing the $Q_P\times Q_S$ spectral Green's functions is obtained from the last equation as

$$\mathbf{X}=\mathbf{L}^T\mathbf{T}(\mathbf{S}+\lambda^2\mathbf{I})^{-1}\mathbf{T}^{-1}\mathbf{F} \tag{28}$$

where the matrix $\mathbf{L}^T$ is a $Q_P\times N$ matrix that selects the finite-difference grid nodes at the planes at which the spectral Green's function is needed. Since $\mathbf{S}$ is diagonal, it follows immediately from (28) that each element in $\mathbf{X}$ is of the form

$$\hat{A}_z^{e,m}(\lambda,z_i,z_j')=X_{ij}=\sum_{n=0}^{N-1}\frac{P_{in}R_{nj}}{s_n+\lambda^2} \tag{29}$$

where $P_{in}=[\mathbf{L}^T\quad\mathbf{T}]_{in}$ and $R_{nj}=[\mathbf{T}^{-1}\quad\mathbf{F}]_{nj}$. In (29), the constants s_n are dependent only on the properties of the layered medium and the finite-difference grid size. The coefficients P_{in} and R_{nj} depend on both the layered medium properties and the position of the source planes. This step completes the development of the spectral Green's function matrix.

The final step in the construction of the closed-form spatial Green's function involves the calculation of the inverse Fourier-Bessel transform of (29). The relevant integral has the form

$$\mathrm{Int}(s,\rho)=\int_0^\infty\frac{1}{s+\lambda^2}J_0(\lambda\rho)\lambda\,d\lambda \tag{30}$$

where s represents one of the eigenvalues of the matrix $\mathbf{A}$. Using well-known properties of Bessel and Hankel functions [21], the above integral may be cast in the form

$$\mathrm{Int}(s,\rho)=\frac{1}{2}\int_{-\infty}^\infty\frac{1}{s+\lambda^2}H_0^{(2)}(\lambda\rho)\lambda\,d\lambda. \tag{31}$$

Considering this last integral on the complex λ plane, and recognizing that the integrand goes to zero for $\mathrm{Im}\{\lambda\}\to-\infty$, the

residue theorem can be used for its calculation. More specifically, a closed contour that includes the real axis and a circular arc of radius $R \to \infty$ in the lower half of the complex λ plane is used. Since for the case of lossless media the poles corresponding to the guided modes in the structure appear on the real axis, the contour needs to be indented properly (i.e., into the first quadrant for $\mathrm{Re}\{\lambda\} > 0$ and the third quadrant for $\mathrm{Re}\{\lambda\} < 0$). The result of the integration is

$$\mathrm{Int}(s,\rho) = -\frac{\pi i}{2} H_0^{(2)}\left(\sqrt{|s|}\,[\sin(\varphi/2) - i\cos(\varphi/2)]\rho\right) \quad (32)$$

where $\varphi = \arg(s)$ is the argument of the eigenvalue s, which is complex for the case of lossy media. Finally, in view of (32), the inverse Fourier-Bessel transform of (29) is

$$A_z^{e,m}(\rho, z_i, z_j') = X_{ij} = -\frac{\pi i}{2} \sum_{n=0}^{N-1} P_{in} R_{nj} \cdot H_0^{(2)}\left(\sqrt{|s_n|}\,[\sin(\varphi/2) - i\cos(\varphi/2)]\rho\right). \quad (33)$$

For the case where s_n is real positive ($\varphi = 0$), the relationship

$$K_0\left(\sqrt{s_n}\rho\right) = -\frac{\pi i}{2} H_0^{(2)}\left(-i\sqrt{|s_n|}\rho\right) \quad (34)$$

is used to rewrite the relevant terms in (31) in terms of the modified Bessel function K_0. This completes the development of the closed-form expression for the vector potential A_z^e or A_z^m. Once expressions for the potentials are available, the field components can be obtained using (2) and (3). Herewith, derivatives with respect to z are calculated numerically, while the derivatives with respect to x and y can be carried out analytically.

III. The Case of the Horizontal Dipole Excitation

The development of the Green's function due to a horizontal electric dipole (HED) or a horizontal magnetic dipole (HMD) located at $z = z'$ inside a layered medium is more complicated than that for the vertical dipole. Without lose of generality, the dipole with moment $I^{e,m}l$ is located at $x = y = 0$ and oriented in the x-direction. As it was pointed out by Sommerfeld, for the field boundary conditions at the planar media interfaces to be met, both the x- and z-components of the vector potential are required. This choice is not unique, and other vector potential function selections are possible [2]. For the purposes of this paper, Sommerfeld's traditional approach of working with the x and z components of the vector potential is chosen. The development is for the case of an HED. A similar approach can be followed for the case of an HMD. The relevant Helmholtz equations for A_x^e and A_z^e are

$$\nabla^2 A_x^e + k^2 A_x^e = -j_x^e \quad (35)$$

$$\nabla^2 A_z^e + k^2 A_z^e = 0. \quad (36)$$

Once again, the following Bessel-Fourier transform pair is used for A_x^e and A_z^e:

$$\hat{A}_{x,z}^e(\lambda, z, z') = \int_0^\infty A_{x,z}^e(\rho, z, z') J_0(\lambda\rho)\rho\, d\rho \quad (37a)$$

$$A_{x,z}^e(\rho, z, z') = \int_0^\infty \hat{A}_{x,z}^e(\lambda, z, z') J_0(\lambda\rho)\lambda\, d\lambda. \quad (37b)$$

Introducing the auxiliary potential $\Lambda_z^e(\rho, z, z')$ such that

$$A_z^e(\rho, z, z') = \frac{\partial \Lambda_z^e(\rho, z, z')}{\partial x} \quad (38)$$

and its Fourier-Bessel transform, the system of (35) and (36) assumes the following form in the spectral domain:

$$\frac{d^2 \hat{A}_x^e}{dz^2} + (k^2 - \lambda^2)\hat{A}_x^e = -\frac{I_x^e l}{2\pi}\,\delta(z - z') \quad (39)$$

$$\frac{d^2 \hat{\Lambda}_z^e}{dz^2} + (k^2 - \lambda^2)\hat{\Lambda}_z^e = 0. \quad (40)$$

The relevant boundary conditions at the conducting planes and media interfaces are given below

$$\hat{A}_x^e\Big|_{\substack{z=0\\z=d}} = 0 \quad (41)$$

$$\hat{A}_x^e\Big|_{z=z_i-} = \hat{A}_x^e\Big|_{z=z_i+} \quad (42)$$

$$\frac{d\hat{A}_x^e}{dz}\bigg|_{z=z_i-} = \frac{d\hat{A}_x^e}{dz}\bigg|_{z=z_i+} \quad (43)$$

$$\frac{d\hat{\Lambda}_z^e}{dz}\bigg|_{\substack{z=0\\z=d}} = 0 \quad (44)$$

$$\hat{\Lambda}_z^e\Big|_{z=z_i-} = \hat{\Lambda}_z^e\Big|_{z=z_i+} \quad (45)$$

$$\frac{1}{\varepsilon_{i-1}}\left[\hat{A}_x^e + \frac{d\hat{\Lambda}_z^e}{dz}\right]\bigg|_{z=z_i-} = \frac{1}{\varepsilon_i}\left[\hat{A}_x^e + \frac{d\hat{\Lambda}_z^e}{dz}\right]\bigg|_{z=z_i+}. \quad (46)$$

Condition (46) is the one providing coupling between A_x^e and A_z^e due to the presence of the discontinuity in the dielectric properties of adjacent layers.

The development of the discrete approximation of (39) and (40) follows closely that presented earlier for the vertical dipole. The primary difference is that due to the coupling of the two components of the vector potential, the vector of unknowns contains the discrete values of both A_x^e and $\hat{\Lambda}_z^e$. Boundary conditions (41)–(45) get incorporated into the scheme in the same way as for the case of the vertical dipole [see (7)–(12)].

From (46), it is apparent that the first derivative of $\hat{\Lambda}_z^e$ is discontinuous at the interface. Consequently, (40) is satisfied everywhere except for the points at the interfaces. Thus, these points will be excluded from the vector of unknowns $\hat{\Lambda}_z^e(z_q)$. Following the same procedure used for the enforcement of boundary condition (9) for the vertical dipole, a discrete form of boundary condition (46) is used to derive finite-difference equations for the points just above and below the media interface point z_q

$$\frac{\hat{\Lambda}_z^e(z_{q+2}) - 2\hat{\Lambda}_z^e(z_{q+1})}{h^2} + \frac{\left[\dfrac{\varepsilon_-\hat{\Lambda}_z^e(z_{q+1})}{\varepsilon_- + \varepsilon_+} + \dfrac{\varepsilon_+\hat{\Lambda}_z^e(z_{q-1})}{\varepsilon_- + \varepsilon_+} - h\,\dfrac{\varepsilon_+ - \varepsilon_-}{\varepsilon_- + \varepsilon_+}\,\hat{A}_x^e(z_q)\right]}{h^2} + (k_0^2\varepsilon_+ - \lambda^2)\hat{\Lambda}_z^e(z_{q+1}) = 0 \quad (47)$$

and

$$\frac{\hat{\Lambda}_z^e(z_{q-2}) - 2\hat{\Lambda}_z^e(z_{q-1})}{h^2} + \frac{\left[\dfrac{\varepsilon_-\hat{\Lambda}_z^e(z_{q+1})}{\varepsilon_- + \varepsilon_+} + \dfrac{\varepsilon_+\hat{\Lambda}_z^e(z_{q-1})}{\varepsilon_- + \varepsilon_+} - h\,\dfrac{\varepsilon_+ - \varepsilon_-}{\varepsilon_- + \varepsilon_+}\,\hat{A}_x^e(z_q)\right]}{h^2} + (k_0^2\varepsilon_- - \lambda^2)\hat{\Lambda}_z^e(z_{q-1}) = 0. \tag{48}$$

The resulting system of discrete equations assumes the following matrix form:

$$\left\{\begin{bmatrix}\mathbf{A}_{xx} & \mathbf{0}\\ \mathbf{A}_{zx} & \mathbf{A}_{zz}\end{bmatrix} + \lambda^2\begin{bmatrix}\mathbf{I} & \mathbf{0}\\ \mathbf{0} & \mathbf{I}\end{bmatrix}\right\}\cdot\begin{bmatrix}\mathbf{x}_x\\ \mathbf{x}_z\end{bmatrix} = \begin{bmatrix}\mathbf{Fu}\\ \mathbf{0}\end{bmatrix} \tag{49}$$

where the (coupling) block $\mathbf{A}_{zx}$ contains nonzero entries only for grid points adjacent to material interfaces. The matrix $\mathbf{F}$ is defined in exactly the same manner as was done for the case of the vertical dipole to account for all sources for which the Green's function must be generated. A compact form of (49) is

$$(\mathbf{B} + \lambda^2\mathbf{I})\mathbf{x} = \mathbf{Gu} \tag{50}$$

where $\mathbf{x}^T = [\mathbf{x}_x^T \;\; \mathbf{x}_z^T]$. Matrix $\mathbf{B}$ is not tridiagonal anymore because of the coupling between the two vector potential components. Nevertheless, following the same procedure as for the vertical dipole, the eigen-decomposition of $\mathbf{B}$ is used in the formal matrix solution of (50) to yield pole-residue representations for the spectral domain forms of the vector potential components at the nodes of the finite-difference grid. Thus, using the notation for the vertical dipole [see (28) and (29) and the relevant discussion], the potentials at a given node in the finite-difference grid due to a source at node j are given by

$$\left.\begin{array}{ll}\hat{A}_x^e(\lambda, z_i, z_j'), & \text{if } 0 \le i,j \le N-3\\ \hat{\Lambda}_z^e(\lambda, z_i, z_j'), & \text{if } N-2 \le i,j \le 2N-\nu-5\end{array}\right\} = \sum_{n=0}^{2N-\nu-5}\frac{P_{in}R_{nj}}{s_n + \lambda^2} \tag{51}$$

where ν is the number of dielectric interfaces present in the layered medium. The index i indicates the row position of the observed quantity in the vector of unknowns. The first $N-2$ quantities are the values of the x component of the vector potential at the interior nodes of the finite-difference grid (recall that this component of the potential is zero at the two conducting planes). The remaining quantities are the values of the auxiliary potential $\hat{\Lambda}_z^e(\lambda, z_i, z_j')$ at the interior nodes of the finite-difference grid. It is noted that the values of the auxiliary potential $\hat{\Lambda}_z^e(\lambda, z_i, z_j')$ at the ν dielectric interfaces are not present in the vector of unknowns since they can be restored from the boundary conditions and the value of $\hat{\Lambda}_z^e(\lambda, z_i, z_j')$ at adjacent grid points. This is also true for the values of the auxiliary potential at the two conducting planes (see (44)).

Substitution of (51) into (37b), followed by an inverse Fourier-Bessel transform operation, yields the desired closed-form expressions for the potentials A_x^e and A_z^e in the spatial domain

$$A_x^e(\rho, z_i, z_j') = -\frac{\pi i}{2}\sum_{n=0}^{N-\nu-5} P_{in}R_{nj} \cdot H_0^{(2)}\left(\sqrt{|s_n|}\,[\sin(\varphi/2) - i\cos(\varphi/2)]\rho\right), \quad 0 \le i,j \le N-3 \tag{52}$$

and

$$A_z^e(\rho, z_i, z_j') = -\frac{\pi i}{2}\sum_{n=1}^{N-\nu-5} P_{in}R_{nj} \cdot \frac{\partial}{\partial x}H_0^{(2)}\left(\sqrt{|s_n|}\,[\sin(\varphi/2) - i\cos(\varphi/2)]\rho\right), \quad N-2 \le i,j \le 2N-\nu-5. \tag{53}$$

This step completes the development of closed-form expressions for the magnetic vector potentials generated by horizontal dipoles in layered media bounded above and below by a pair of conducting planes. Expressions for the electric and magnetic fields may be derived from the above expressions using (2) and (3). In doing so, derivatives with respect to z are to be taken numerically, while transverse derivatives with respect to x and y are calculated analytically.

Before we proceed with the numerical validation of the method, it is appropriate to consider the computational cost associated with the calculation of the closed-form expressions of (33), (52), and (53). From these expressions, it is clear that the number of terms involved in the associated sums is equal to the number of discrete unknowns in the finite-difference approximation. However, in the numerical implementation of the proposed method, model order reduction is used to reduce this number. Such model order reduction is prompted by the fact that only a subset of the calculated discrete eigenvalues of the finite-difference matrices $\mathbf{A}$ (for the case of the vertical dipole) and $\mathbf{B}$ (for the case of the horizontal dipole) is calculated accurately, and it is only this subset of eigenvalues that contributes significantly to the solution. Consequently, a Krylov subspace method based on the Arnoldi algorithm is used to reduce the number of terms in the closed-form expressions of (33), (52), and (53) [24].

The details of the associated eigenvalue order reduction algorithm can be found in [20], [23], and [24] and will not be repeated here. We only make the following comments. First, given the grid size h, the properties of the media, and the frequency of interest, error estimates for the eigenvalues of the discrete eigenvalue problem can be used to guide the selection of the number of terms in the reduced sums for the closed-form expressions of (33), (52), and (53) [25]. Second, our numerical experiments indicate that very accurate results are obtained using reduced sums with a number of terms on the order of one-fifth of the number of unknowns in the discrete finite-difference problem if the radial distance ρ between dipole and point of observation is larger than $0.2\lambda_0$, where λ_0 is wavelength in free space. For smaller distances, a robust criterion for the number of terms in the reduced model that suffice for acceptable accuracy has not been derived yet. Thus, at this point, model order reduction is not performed for the calculation of the Green's functions for

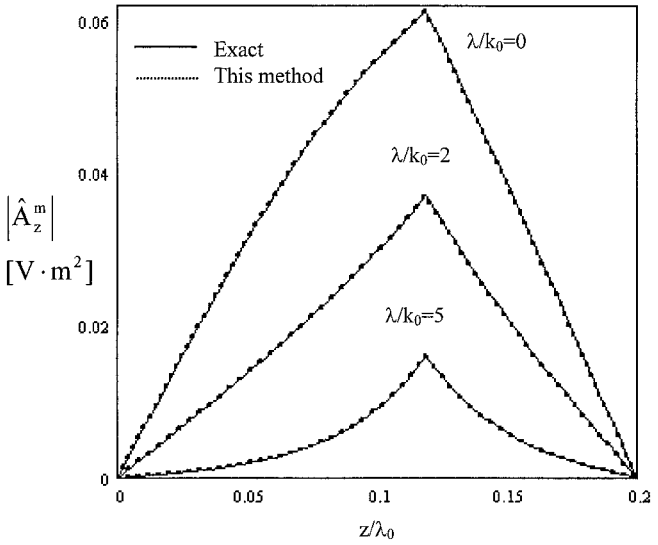

Fig. 2. Magnitude of the spectrum of the z-component of the magnetic vector potential versus distance along the media cross section.

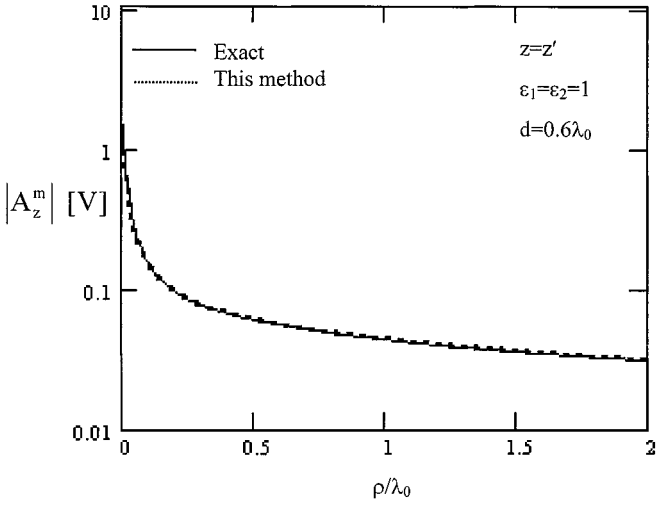

Fig. 3. Magnitude of the z-component of the magnetic vector potential versus radial distance from the dipole along the plane of the dipole. The homogeneous medium enables comparison with the analytic solution.

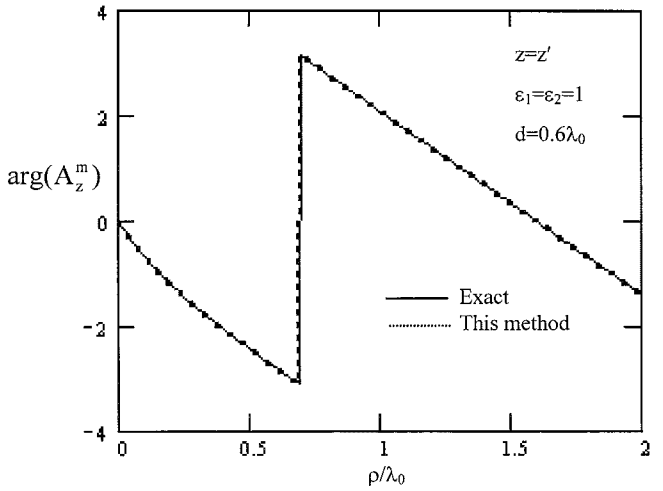

Fig. 4. Argument of the z-component of the magnetic vector potential versus radial distance from the dipole along the plane of the dipole. The homogeneous medium enables comparison with the analytic result.

distances less than $0.2\lambda_0$ from the source. This issue is currently under investigation, and ways to reduce the computational cost of the calculation of the Green's function at short distances from the sources will be reported in a forthcoming paper.

IV. Numerical Analysis and Validation of Results

The following numerical studies involve the application of the proposed methodology for the calculation of the Green's function for a vertical magnetic dipole and a horizontal electric dipole located in a shielded layered substrate. Validation is effected through comparisons of the results obtained using the proposed methodology with those obtained either analytically for the spectra of the potentials or from the calculation of the Sommerfeld integrals for the space-domain forms of the potential using DCIM.

The first study involves a VMD inside a two-layer substrate between two conducting plates set at a distance $d = 0.2\lambda_0$, where λ_0 is the wavelength in free space. The bottom layer is of thickness $0.1\lambda_0$ with relative permittivity of 2.5. The relative permittivity of the top layer is 1. The magnetic moment of the dipole is such that $I_z^m l/k_0 = 1$ [V · m^2]. The dipole is placed at $z = 0.12\lambda_0$. Fig. 2 depicts the magnitude of the spectrum of the magnetic vector potential $\hat{A}_z^m(\lambda, z, z')$, calculated for different values of the spectral variable λ versus z. Excellent agreement is observed between the results obtained using the proposed method and analytical methods.

For the case of a homogeneous dielectric, an analytic solution is also available for the vector potential in the spatial domain

$$A_z^m(\rho, z, z') = \frac{I_z^m l}{\pi d} \sum_{n=1}^{\infty} \sin\frac{n\pi z}{d} \sin\frac{n\pi z'}{d} K_0(\beta_n \rho) \quad (54)$$

where K_0 is the modified Bessel function of zeroth order and $\beta_n = \sqrt{(n\pi/d)^2 - k_0^2\varepsilon}$. The second example considered deals with such a case of a homogeneously filled, parallel-plate guide. The plate separation is taken to be $0.6\lambda_0$ with the relative permittivity of the medium set equal to one. The plate separation is such that the mode TE_z is excited. The magnetic dipole moment was taken $I_z^m(k_0 l) = 1$ [V]. Figs. 3 and 4 depict the calculated spatial vector potential in magnitude and phase, respectively, versus the distance from the dipole on the plane that contains the dipole. The results are in very good agreement with those obtained from the analytic expression (54).

Next, the case of an HED is considered. The dipole is placed inside a two-layer medium, each of thickness $0.1\lambda_0$, and relative permittivities of $\varepsilon_{r1} = 1$ for the top layer and $\varepsilon_{r2} = 12.6$ for the bottom layer. The separation between the top and bottom conducting plates was taken to be $d = 0.2\lambda_0$. The dipole was placed at the interface between the two dielectrics, and its moment was assumed to be such that $I_x^e l W_0 k_0^2 = 1$ [V/m], where W_0 is the intrinsic impedance of free space. Figs. 5 and 6 compare the spectrums $\hat{A}_x^e$ and $\hat{A}_z^e$ obtained by the proposed and analytic methods. Very good accuracy is observed. The accuracy in this case is strongly dependent on the grid size. This is attributed to the way the coupling between the two potential components occurs, namely, through the enforcement of the tangential field continuity at the media interfaces. Our experiments have shown that use of a fine grid leads to very good accuracy

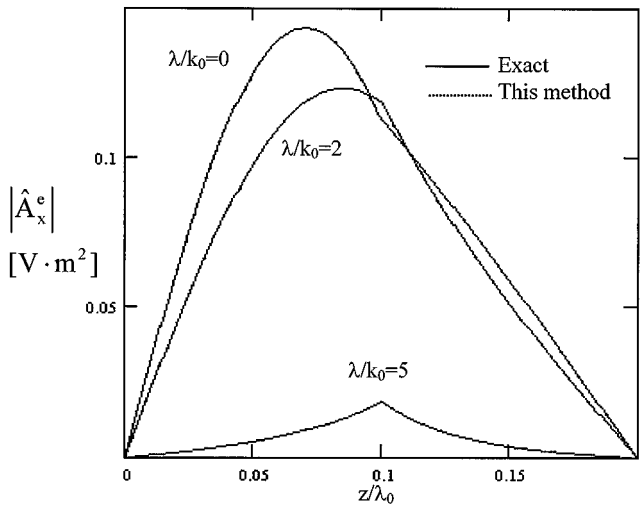

Fig. 5. Magnitude of the spectrum of the x-component of the electric vector potential versus z for different values of the spectral variable λ.

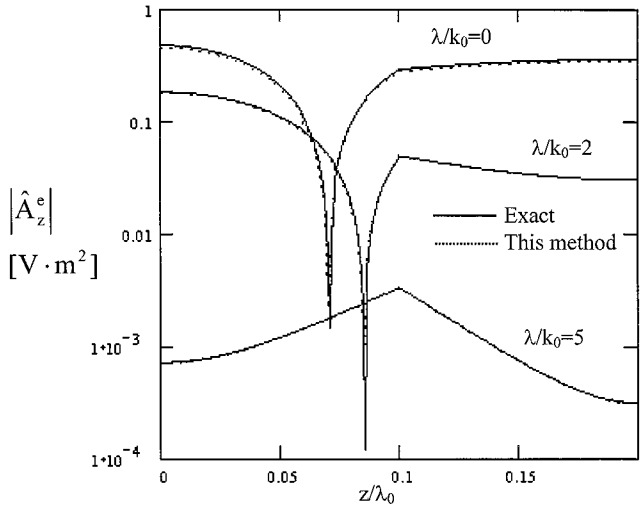

Fig. 6. Magnitude of the spectrum of the z-component of the electric vector potential versus z for different values of the spectral variable λ.

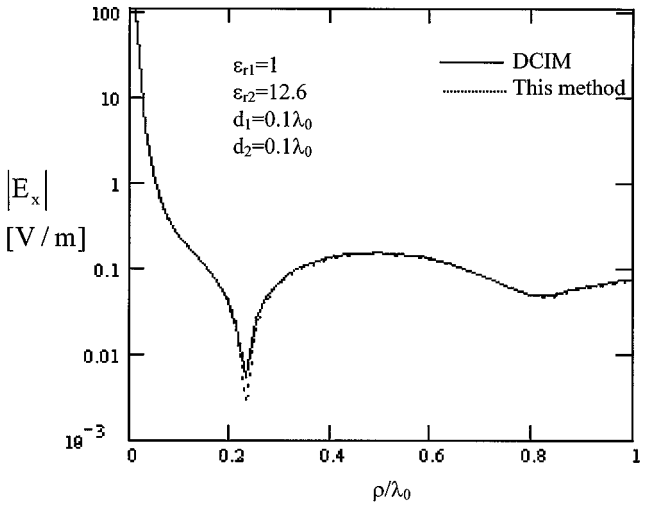

Fig. 7. Magnitude of the x-component of the electric field due to an x-oriented electric dipole. The field is calculated along the plane of the dipole.

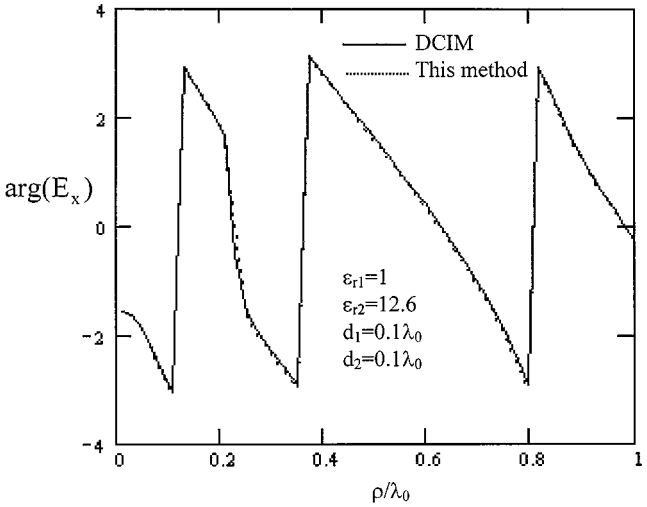

Fig. 8. Argument of the x-component of the electric field due to an x-oriented electric dipole. The field is calculated along the plane of the dipole.

in the approximation of the spectra of the potentials. For the specific case considered in this example, 300 grid points were used in the finite-difference grid. Clearly, it is for such cases that model order reduction is necessary to keep the number of terms in the finite sums of (52) and (53) small.

Figs. 7 and 8 depict the comparison of the results obtained using the proposed method for the electric field in space with the results obtained from the application of DCIM. More specifically, the magnitude and phase of the x-component of the electric field along the plane of the horizontal dipole is examined. The DCIM calculation was based on the formulation of [6] and the calculation of the Sommerfeld integral using the modified path described in [5]. Once again, very good agreement is observed. Further experimentation with the proposed methodology, using source and observation position and layered substrate properties as parameters, proved the method to be robust and accurate.

V. Conclusions

This paper has proposed a new approach for the direct development of closed-form spatial Green's functions for electromagnetic problems in shielded, planar, multilayered media. The closed-form expression is in terms of a finite sum of Hankel functions of the second type and zeroth order. Unlike the discrete complex image method, the proposed methodology does not require the extraction of the poles of the spectra of the Green's functions. Once the source and observation planes have been identified, all required Green's functions are generated simultaneously. The z-plane location of the source and observation points is embedded in the coefficients of the resulting finite sums, while the radial dependence appears in the argument of the Hankel functions in the form $(s_n)^{1/2}\rho$, where the constants s_n depend on the properties of the layered medium.

The proposed methodology is applicable to both vertical and horizontal dipoles. For the horizontal dipole case, the Sommerfeld choice of the vector potentials was used. Samples of our

preliminary numerical experiments were presented to demonstrate the validity and accuracy of the proposed methodology. Further studies are currently in progress, aimed at better understanding of the impact of the finite-difference grid size on the accuracy of the generated closed-form expressions for the Green's functions. The finer the grid size, the larger the number of terms present in the closed-form expression. Currently, model order reduction is used to reduce the number of terms in the closed-form expressions by keeping only the significant eigenvalues in the finite-difference approximation of the differential equations of the spectra of the vector potentials. Our preliminary studies have shown that for distances from the source point greater than one-fifth of the free-space wavelength, a reduced model of order equal to one-fifth of the number of discrete unknowns is sufficient for excellent accuracy. However, this is not the case for shorter distances. Thus, our ongoing studies are also aimed at methodologies alternative to model order reduction for expediting the calculation of the finite sum of Hankel functions that constitutes the closed form of the Green's function.

Even though the proposed methodology was presented for the case of shielded, planar, multilayered substrates, its extension to the unshielded case is possible and will be the topic of a forthcoming paper.

REFERENCES

[1] J. R. Mosig, "Integral equation techniques," in *Numerical Techniques for Microwave and Millimeter-Wave Passive Structures*, T. Itoh, Ed. New York: Wiley, 1988.

[2] K. A. Michalski and D. Zheng, "Electromagnetic scattering and radiation by surfaces of arbitrary shape in layered media, Part I: Theory," *IEEE Trans. Antennas Propagat.*, vol. 38, pp. 335–344, Mar. 1990.

[3] W. C. Chew, *Waves and Fields in Inhomogeneous Media*. Piscataway, NJ: IEEE Press, 1995.

[4] Y. L. Chow, J. J. Yang, D. G. Fang, and G. E. Howard, "A closed-form spatial Green's function for the thick microstrip substrate," *IEEE Trans. Microwave Theory Tech.*, vol. 39, pp. 588–592, Mar. 1991.

[5] M. I. Aksun, "A robust approach for the derivation of closed-form Green's functions," *IEEE Trans. Microwave Theory Tech.*, vol. 44, pp. 651–658, May 1996.

[6] C. Tai, *Dyadic Green Functions in Electromagnetic Theory*. Piscataway, NJ: IEEE Press, 1993.

[7] D. C. Chang and J. X. Zhang, "Electromagnetic modeling of passive circuit elements in MMIC," *IEEE Trans. Microwave Theory Tech.*, vol. 40, pp. 1741–1747, Sept. 1992.

[8] F. Alonso-Monferrer, A. A. Kishk, and A. W. Glisson, "Green's functions analysis of planar circuits in a two-layer grounded medium," *IEEE Trans. Antennas Propagat.*, vol. 40, pp. 690–696, June 1992.

[9] M. J. Tsai, F. D. Flaviis, O. Fordham, and N. G. Alexopoulos, "Modeling planar arbitrary shaped microstrip elements in multilayered media," *IEEE Trans. Microwave Theory Tech.*, vol. 45, pp. 330–337, Mar. 1997.

[10] Q.-H. Liu and W. C. Chew, "Application of the conjugate gradient fast Fourier Hankel transfer method with an improved fast Hankel transform algorithm," *Radio Sci.*, vol. 29, pp. 1009–1022, July–Aug. 1994.

[11] R. C. Hsieh and J. T. Kuo, "Fast full-wave analysis of planar microstrip circuit elements in stratified media," *IEEE Trans. Microwave Theory Tech.*, vol. 46, pp. 1291–1297, Sept. 1998.

[12] T. J. Cui and W. C. Chew, "Fast evaluation of Sommerfeld integrals for EM scattering and radiation by three-dimensional buried objects," *IEEE Geosci. Remote Sensing*, vol. 37, pp. 887–900, Mar. 1999.

[13] D. G. Fang, J. J. Yang, and G. Y. Delisle, "Discrete image theory for horizontal electric dipole in a multilayer medium," *Proc. Inst. Elect. Eng. H*, vol. 135, pp. 297–303, Oct. 1988.

[14] J. J. Yang, Y. L. Chow, G. E. Howard, and D. G. Fang, "Complex images of an electric dipole in homogenious and layered dielectrics between two ground planes," *IEEE Trans. Microwave Theory Tech.*, vol. 40, pp. 595–600, Mar. 1992.

[15] F. Ling, D. Jiao, and J. M. Jin, "Efficient electromagnetic modeling of microstrip structures in multilayered media," *IEEE Trans. Microwave Theory Tech.*, vol. 47, pp. 1810–1818, Mar. 1999.

[16] T. K. Sarkar and O. Pereira, "Using the matrix pencil method to estimate the parameters of a sum of complex exponentials," *IEEE Antennas Propagat. Mag.*, vol. 37, pp. 48–55, Feb. 1995.

[17] M. L. Van Blaricum and R. Mittra, "A technique for extracting the poles and residues of a system directly from its transient response," *IEEE Trans. Antennas Propagat.*, vol. AP-23, pp. 777–781, Nov. 1975.

[18] B. Hu and W. C. Chew, "Fast inhomogeneous plane wave algorithm for electromagnetic solutions in layered medium structures—2D case," *Radio Sci.*, vol. 35, no. 1, 2000.

[19] F. Ling, "Fast electromagnetic modeling of multilayer microstrip antennas and circuits," Ph.D. dissertation, Univ. of Illinois , Urbana-Champaign, 2000.

[20] E. J. Grimme, "Krylov projection methods for model reduction," Ph.D. dissertation, Univ. of Illinois, Urbana-Champaign, 1997.

[21] M. Abramovitz and I. Stegun, *Handbook of Mathematical Functions* Dover, U.K., 1965.

[22] W. H. Press, S. A. Teukolsky, W. T. Vetterling, and B. P. Flannery, *Numerical Recipies in Fortran 77*. Cambridge, U.K.: Cambridge Univ. Press, 1992.

[23] R. Freund, "Reduced-order modeling techniques based on Krylov subspaces and their use in circut simulation," in *Numer. Anal. Manuscript 98-3-02*. Murray Hill, NJ: Bell Laboratories, Feb. 1998.

[24] A. Odabasioglu, M. Celik, and L. Pileggi, "PRIMA: Passive reduced-order interconnect macromodeling algorithm," *IEEE Trans. Computer-Aided Design*, vol. 17, pp. 645–654, Aug. 1998.

[25] G. D. Smith, *Numerical Solution of Partial Differential Equations: Finite Difference Methods*. New York: Oxford Univ. Press, 1985.

Andreas C. Cangellaris (M'86–SM'97–F'00) received the diploma from the Aristotle University of Thessaloniki, Greece, in 1981 and the M.S. and Ph.D. degrees from the University of California, Berkeley, in 1983 and 1985, respectively, all in electrical engineering.

From 1985 to 1987, he was a Senior Research Engineer in the Electronics Department of the General Motors Research Laboratories in Warren, MI. From 1987 to 1997, he was with the Department of Electrical and Computer Engineering, University of Arizona, Tucson, first as an Assistant Professor from 1987 to 1992 and then as an Associate Professor from 1992 to 1997. Since 1997, he has been a Professor of electrical and computer engineering at the University of Illinois at Urbana-Champaign. He is an author or coauthor of more than 120 papers in scientific journals and conference proceedings in the areas of computational electromagnetics, modeling and simulation of the electrical performance of high-speed interconnections, and electromagnetic analysis of packaging structures for high-speed electronics. In 1998, he was General Chair for the 8th Biennial Conference on Electromagnetic Field Computation (CEFC) and he is currently serving on the International Steering Committee for this conference.

Prof. Cangellaris is a member of the IEEE Antennas and Propagation Society, the IEEE Microwave Theory and Techniques Society, the IEEE Components, Packaging, and Manufacturing Technology Society, and the IEEE Electromagnetic Compatibility Society. He is a Cofounder of the IEEE Topical Meeting on Electrical Performance of Electronic Packaging. He is an Associate Editor for the IEEE TRANSACTIONS ON ADVANCED PACKAGING and the IEEE Press series on *Electromagnetic Waves*.

Vladimir I. Okhmatovski (M'99) was born in Moscow in 1974. He received the M.S. (with distinction) and candidate of science (Ph.D.) degrees from Moscow Power Engineering Institute, Russia, in 1996 and 1997, respectively.

In 1997, he joined the Radio Engineering Department, Moscow Power Engineering Institute, as an Assistant Professor. From 1998 to 1999, he was a Postdoctoral Fellow at the Microwave Laboratory, National Technical University of Athens, Greece. In 1999, he joined the Department of Electrical and Computer Engineering, University of Illinois at Urbana-Champaign, where he is currently a Postdoctoral Research Associate. He has published more than 15 papers in professional journals and conference proceedings. His research interests include geometrical and physical theories of diffraction, conformal antennas and arrays, fast algorithms in computational electromagnetics, and modeling of high-speed interconnects.

Dr. Okhmatovski received the scholarship of the Government of the Russian Federation in 1995, the scholarship of the President of the Russian Federation in 1996, and the scholarship of the Russian Academy of Science from 1997 to 2000. In 1996, he received the second prize for the best scientist report presentation at the VI International Conference on Mathematical Methods in Electromagnetic Theory (MMET'96).